

DOI: <https://doi.org/10.24425/amm.2024.147795>SANG-HYEON JO¹, SEONG-HEE LEE^{1*}

CHANGES IN MICROSTRUCTURE AND TEXTURE OF A MULTI-STACK ACCUMULATIVE ROLL BONDING PROCESSED COMPLEX ALUMINUM ALLOY WITH ANNEALING

Changes in the microstructure and texture with annealing temperature of a nanostructured complex aluminum alloy fabricated by multi-stack Accumulative Roll Bonding (ARB) process using various Al alloys are investigated in detail. The ARB process is performed up to 4 cycles without lubrication at room temperature. The specimen fabricated by the ARB is a multi-layer aluminum alloy sheet in which the AA1050, AA5052 and AA6061 Al alloys are alternately stacked to each other. The average grain size of the starting material is 140 μm , but after 4 cycles of the ARB process, this is reduced to 150 nm. The complex Al alloy still shows an ultrafine grained microstructure at annealing temperatures up to 250°C, but after annealing at 300°C, it exhibits a heterogeneous structure containing both the ultrafine grains and the coarse grains due to the occurrence of discontinuous recrystallization. The specimens annealed at temperatures above 300 °C also show a heterogeneous microstructure even if the heterogeneities of grain size differ from each other. The texture develops abnormally at higher annealing temperatures; the deformation textures are developed as [112]/ND and [111]/ND components, even in the recrystallized specimens. As the annealing temperature increases, the number fraction of the high-angle grain boundaries gradually decreases. The changes in microstructure and texture of the specimens with increase of the annealing temperature are compared to those of the specimens processed by 2-cycle of the ARB.

Keywords: Multi-stack accumulative roll bonding (ARB); aluminum alloy; microstructure; texture

1. Introduction

Lots of studies on lightweight of automobile have been done because of importance of the energy saving and green environment. In special, the aluminum alloys have been studied extensively because of their benefits such as medium strength, good formability and lightweight [1,2]. It is also expected that the substitution of such aluminum alloys for steels would result in great improvement in energy economy, recyclability and life-cycle cost.

The accumulative roll bonding (ARB) process [3-10], one of the severe plastic deformation processes, is mostly appropriate for practical applications because it can be readily applied by the conventional rolling process. Previous studies have demonstrated that the ultra-grain refinement by the ARB process can be efficiently attained for various metallic materials such as aluminum alloys [3-7] and copper alloys [8-11]. This has shown that it is not necessary to utilize the same materials in the ARB process. Therefore, the ARB of dissimilar materials rather than of the same ones, has recently been actively studied. This modified ARB has the merit of being able to fabricate various

metal/metal multi-layer composite materials with heterogeneous microstructure, and improve the mechanical properties. However, most of the studies were of the ARB of different kinds of metallic materials such as Al and Cu [12], Al and Mg [13], and Al and Ni [14]. However, the studies of the ARB of dissimilar alloys of the same metal have seldom been performed [15-17].

It is expected that the ARB of dissimilar alloys of the same metal would enable the production of unique alloys that consist of more complex and various microstructure such as the heterogeneous microstructure in which the grains of nanometer and micrometer order coexist together, resulting in enhancing the mechanical properties of the aluminum alloys. In particular, complex Al alloys having various mechanical properties can be fabricated by the ARB, as reported in previous studies [15-18]. In this way, if the stacking number was increased per ARB cycle, ultrafine grain refinement would be attained very effectively. The authors also report in previous study the changes in microstructure and mechanical properties of the AA1050/AA5052/AA6061/AA1050 alloys fabricated by two cycles of the multi-stack ARB with annealing temperature [19,20]. The study found that heterogeneous microstructure consisting of both

¹ MOKPO NATIONAL UNIVERSITY, ADVANCED MATERIALS SCIENCE AND ENGINEERING, MUAN-GUN, JEONNAM 58554, KOREA

* Corresponding author: shlee@mokpo.ac.kr



fine and coarse grains could be developed in the complex Al alloy through the ARB and subsequent annealing [20], however, ultrafine grains did not develop due to the lack of ARB cycles. Therefore, in this study, the ARB process was repeated up to four cycles. In general, the equivalent strain ($\bar{\varepsilon}$) introduced by the ARB process is calculated by the following equation [7],

$$\bar{\varepsilon} = \frac{2}{\sqrt{3}} n \ln k$$

where, n and k are the number of ARB cycles and the number of stacking, respectively. The value of k is equal to 4 due to the 4-layer stack ARB in both cases, regardless of the number of ARB cycles. However, the value of n differs as 2 and 4 for 2 and 4 cycles, respectively. Thus, the equivalent strain in this study is as large as 6.4, equal to that of 8 cycles in the 2-layer stack ARB, and twice that ($=3.2$) of the previous study. Therefore, it is estimated that the changes in microstructure with increasing the annealing temperature will be significantly different. In this study, the changes in microstructure and texture with annealing of a nanostructured aluminum alloy fabricated by 4 cycles of multi-stack ARB process using different Al alloys were investigated in detail.

2. Experimental

The materials used in this study were commercial purity AA1050, AA5052 and AA6061 sheets with thickness of 2 mm,

of which TABLE 1 shows the compositions. The as-received AA1050, AA5052, and AA6061 alloys were annealed at 500°C for 1 hour, to remove the stored strain remaining in the materials. Fig. 1 shows the microstructures of the starting materials and a schematic of the ARB process. The average grain size of the AA6061, AA5052, and AA1050 alloys was (29, 39, and 72) μm , respectively. As shown in the inverse pole figures, the AA5052 and AA1050 alloys exhibited recrystallization texture in which the $\{100\}$ //ND component mainly developed, while AA6061 alloy had a rolling texture in which the $\{110\}$ //ND component developed.

For the ARB process, the Al alloy sheets were cut into dimensions of 50 mm width \times 200 mm length. The AA1050, AA5052, and AA6061 sheets were alternately stacked by four layers after wire-brushing, and roll-bonded to 2 mm in thickness by multi-pass rolling at ambient temperature. This AA1050/AA5052/AA6061/AA1050 complex Al sheet was then stacked into and reduced to 2 mm in thickness by the same procedure, as shown in Fig. 1. The ARB process was performed up to 4 cycle (c), without lubrication. The as-rolled specimens were then annealed for 0.5 h at various temperatures from (200 to 500)°C. The microstructure and texture of the specimens were analyzed by SEM/EBSD (electron back scattering diffraction) measurement. The EBSD measurement was carried out using the program TSL OIM Data Collection ver.3.5 in Phillips XL30s SEM with FE-gun operated at 20 kV. The EBSD analysis was conducted using the program TSL OIM Analysis ver. 3.0.

TABLE 1

Chemical compositions of the AA1050, AA6061 and AA5052 alloys studied (wt. %)

Materials	Si	Fe	Cu	Mn	Mg	Cr	Zn	Ti	Each	Al
AA1050	0.03	0.29	0.02	0.01	0.01	-	0.01	0.009	0.03	RE
AA6061	0.6	0.7	0.3	0.15	1.0	0.155	0.25	0.15	0.05	RE
AA5052	0.21	0.273	0.028	0.069	2.26	0.162	0.028	-	0.05	RE

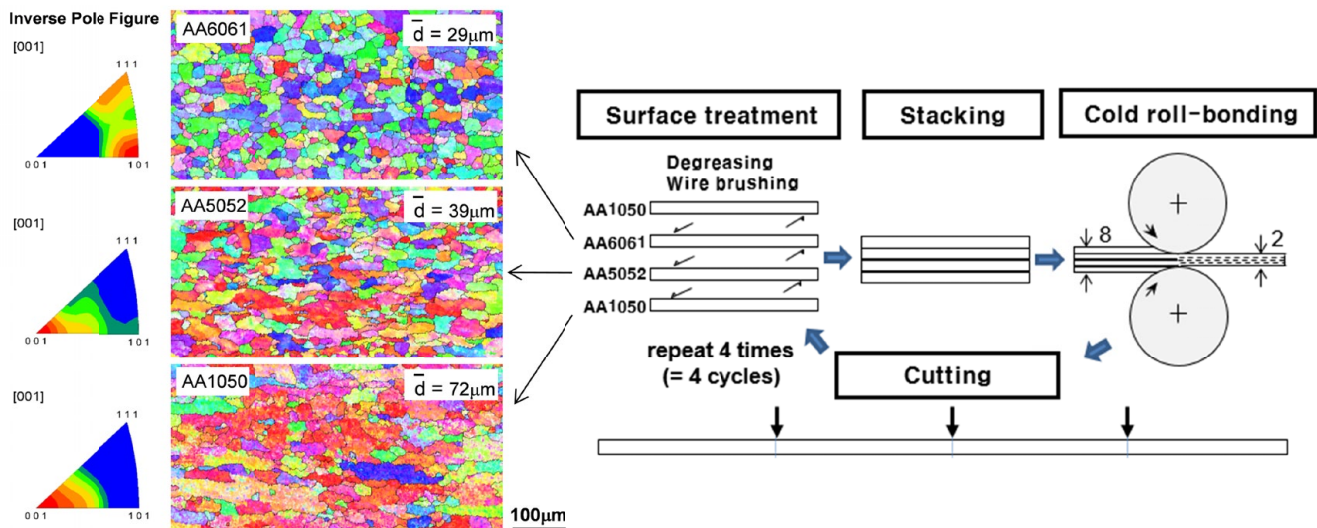


Fig. 1 Microstructure of starting materials and schematic of the multi-stack accumulative roll-bonding (ARB) process studied

3. Results and discussion

The ARB process up to 4c was successfully performed without any shape defects. Fig. 2 shows the normal direction (ND) map, the rolling direction (RD) map, and the grain boundary (GB) map obtained from EBSD measurement of the as-ARB-processed and subsequently annealed specimens. The color of each point indicates the crystallographic direction parallel to ND and RD of the specimens, corresponding to the colored. The as-ARB-processed specimen showed an ultrafine grained structure with average grain diameter of 150 nm, as shown in the figure. This indicates that the ultra-grain refinement was successfully attained by 4c of the multi-stack ARB, different from the 2c ARB in the previous study [20]. From the inverse pole figure, it is found that $\{110\}$ //ND texture, a component of deformation texture, developed. In addition, it is clear from the GB map that the high-angle grain boundaries (HAGB) above 15 degrees have higher volume fraction than the low-angle grain boundaries (LAGB) below 15 degrees. The specimen annealed at 200°C still shows a typical ultrafine grained structure even though the grain size increases slightly due to the occurrence of static recovery. However, for the 300°C annealed specimen, the static recrystallization occurred actively along the rolling direction, as indicated by the arrows in Fig. 2. Here, it is very interesting that the recrystallization occurred mainly along the rolling direc-

tion. We cannot affirm where the recrystallization took place, because the various aluminum alloys are intermixed. However, it is probable that the recrystallized regions belong to the material with low recrystallization temperature such as the AA1050. This static recrystallization occurred more actively after annealing at 400°C, so that all regions of the specimen were completely recrystallized. However, the grain diameter differed depending on the region. That is, it exhibited a heterogeneous structure in which the various kinds of grains coexisted together. This heterogeneous microstructure was still observed in the specimen annealed at 500°C though the grain size distribution differed from that of 400°C, as shown in Fig. 2. It was clearly found that these changes in microstructure with increasing the annealing temperature were greatly different from those of specimen processed by 2c of the ARB in the previous study. In addition, it was found from the GB map that as the annealing temperature increased, the fraction of HAGBs gradually decreased.

Here, the changes in texture with increasing the annealing temperature were also very interesting. The specimens until 250°C still showed still a deformation texture that was similar to that of the as-rolled material. However, the texture development of specimens above 300°C was changed due to the static recrystallization. Fig. 3 shows the change in texture components with increasing the annealing temperature. The specimen annealed at 300°C had both the $[001]$ //ND component of typical

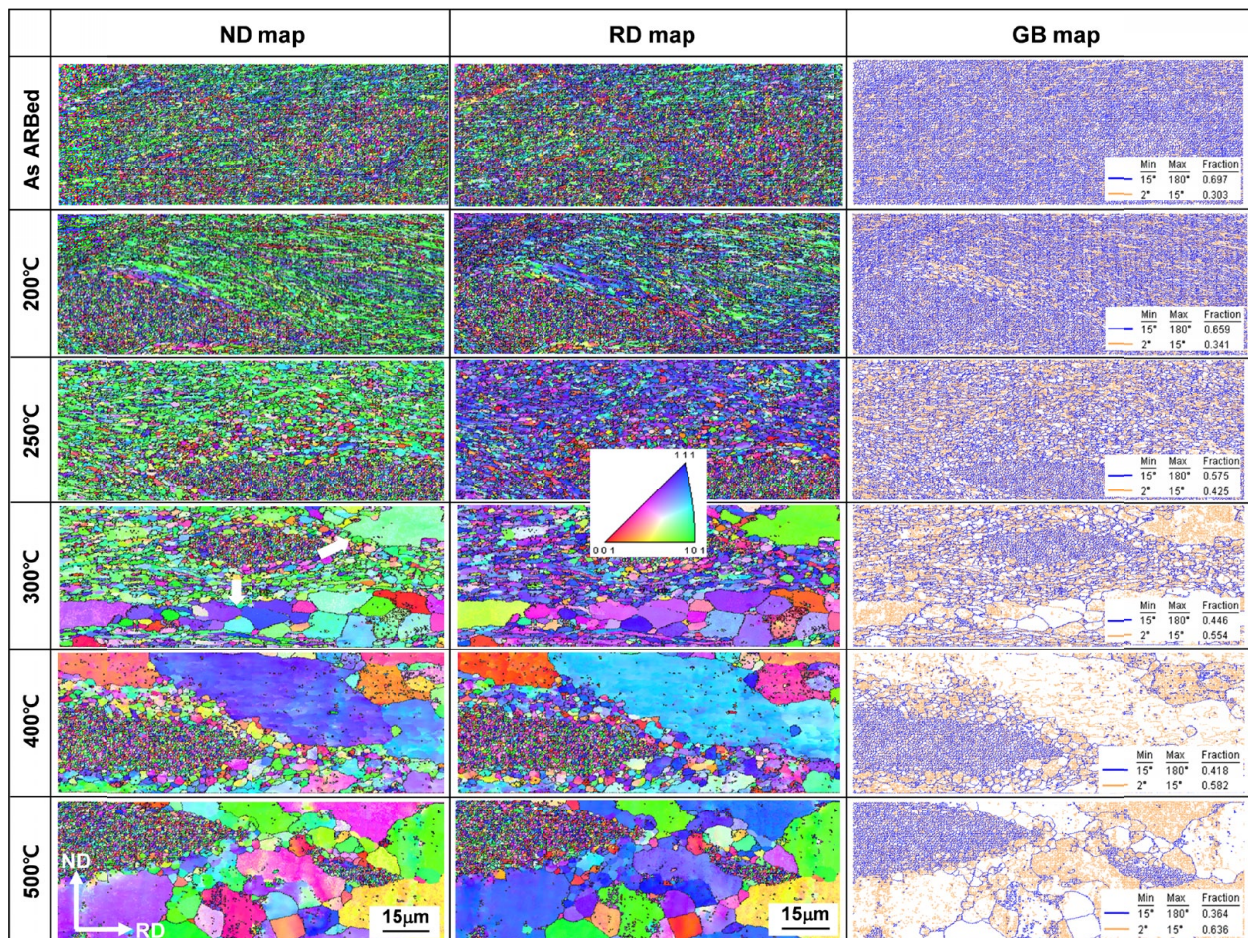


Fig. 2 ND, RD and GB maps of the specimens processed by 4c of the multi-stack ARB and subsequently annealed at various temperatures

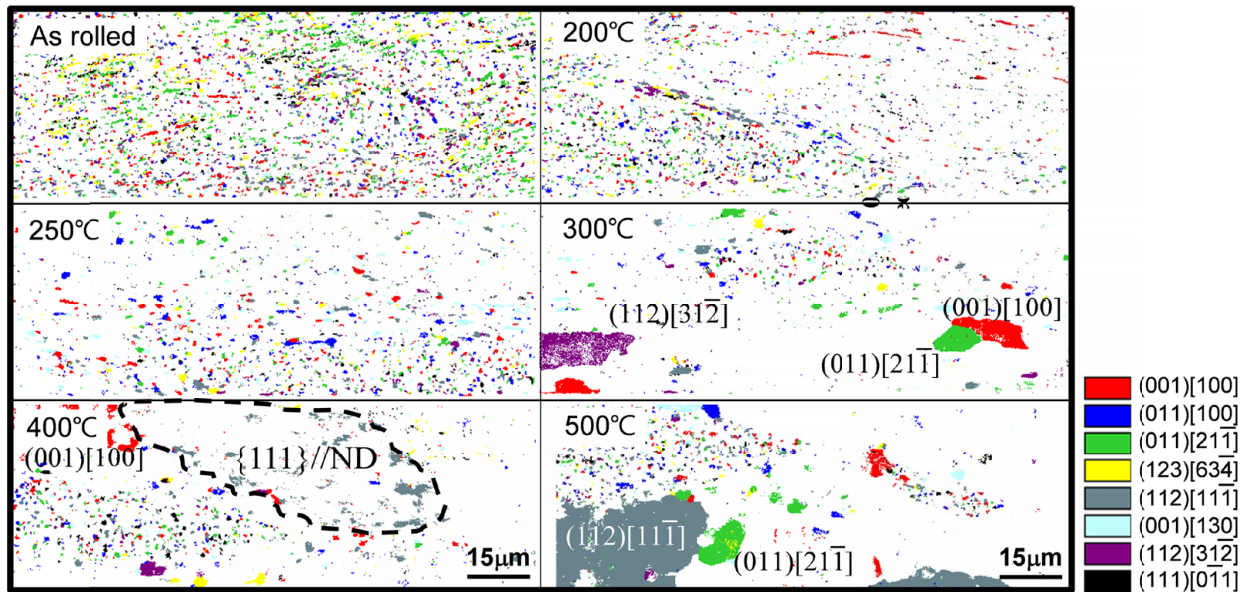


Fig. 3 Textural development of the specimens processed by 4c of the multi-stack ARB and subsequently annealed at various temperatures

recrystallization texture, and the $[112]//ND$ and $[011]//ND$ components of the rolling texture. The development of these abnormal textures was also observed at the specimens above 400°C . That is, the $[112]//ND$ and $[111]//ND$ components that are rarely seen in the recrystallized Al alloys developed in the specimens annealed at (400 and 500°C), respectively. Fig. 4 shows the changes in the volume fraction of texture components with increasing the annealing temperature. As shown in the figure, up to 400°C , there was no significant difference in the volume fraction even if the temperature increased. However, the volume fraction of the $(112)[11\bar{1}]$ component, the conventional rolling texture, was overwhelmingly high in the specimen annealed at 500°C , compared to those of the other components. In general, the recrystallization texture such as the $\{001\}\langle 100\rangle$ component develops in the specimens annealed at higher temperatures, as

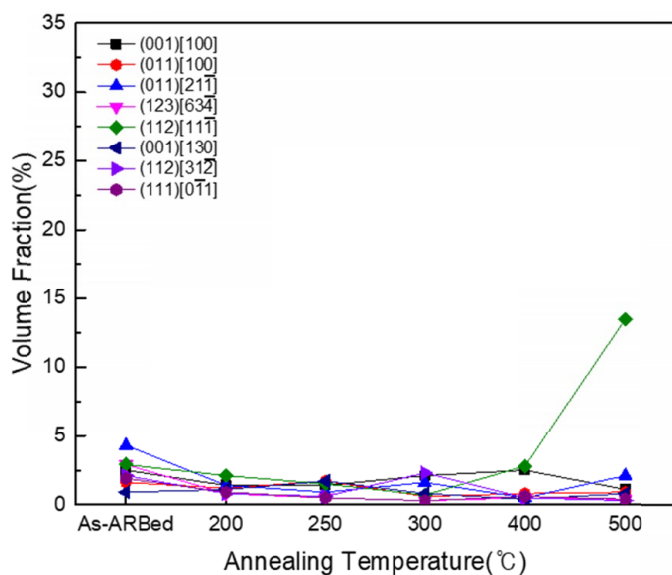


Fig. 4 Changes in the volume fraction of texture components with increasing the annealing temperature

shown in previous study [20]. Here, the reason why a kind of abnormal texture developed in the specimen annealed at 500°C is probably that the specimen was severely plastic deformed by 4c of the multi-stack ARB before annealing.

Fig. 5 shows the misorientation distribution of the grain boundaries obtained from the results of EBSD measurement for the specimens annealed at various temperatures. As shown in the figure, the number fraction of the HAGBs tended to decrease with the increase of annealing temperature. In particular, LAGBs below 10 degrees showed an overwhelming fraction for the specimens above 300°C . This suggests that the recrystallized grains contain lots of dislocation cells and/or subgrains even after the static recrystallization. This specific microstructure is sometimes observed in the specimens severely deformed by the ARB. In addition, it is well known that this decreases the ductility in the specimens annealed after the multi-stack ARB process.

4. Conclusions

Changes in the microstructure and textures of a nanostructured complex aluminum alloy fabricated by 4c of the multi-layer stack ARB process using different Al alloys such as AA1050, AA5052 and AA6061 alloy sheets with increasing the annealing temperature were investigated in detail. After the ARB of 4 cycles, the average grain diameter was 150 nm. The specimen annealed at 200°C still showed a typical ultrafine grained structure, however, after 300°C , discontinuous static recrystallization began to occur, while above 400°C , the specimen exhibited heterogeneous microstructure in which the various recrystallized grains coexisted together over wide regions. In addition, increasing temperature tended to decrease the number fraction of high-angle boundaries. The rolling texture such as $[112]//ND$ and $[111]//ND$ also developed even in the specimens annealed at higher temperatures.

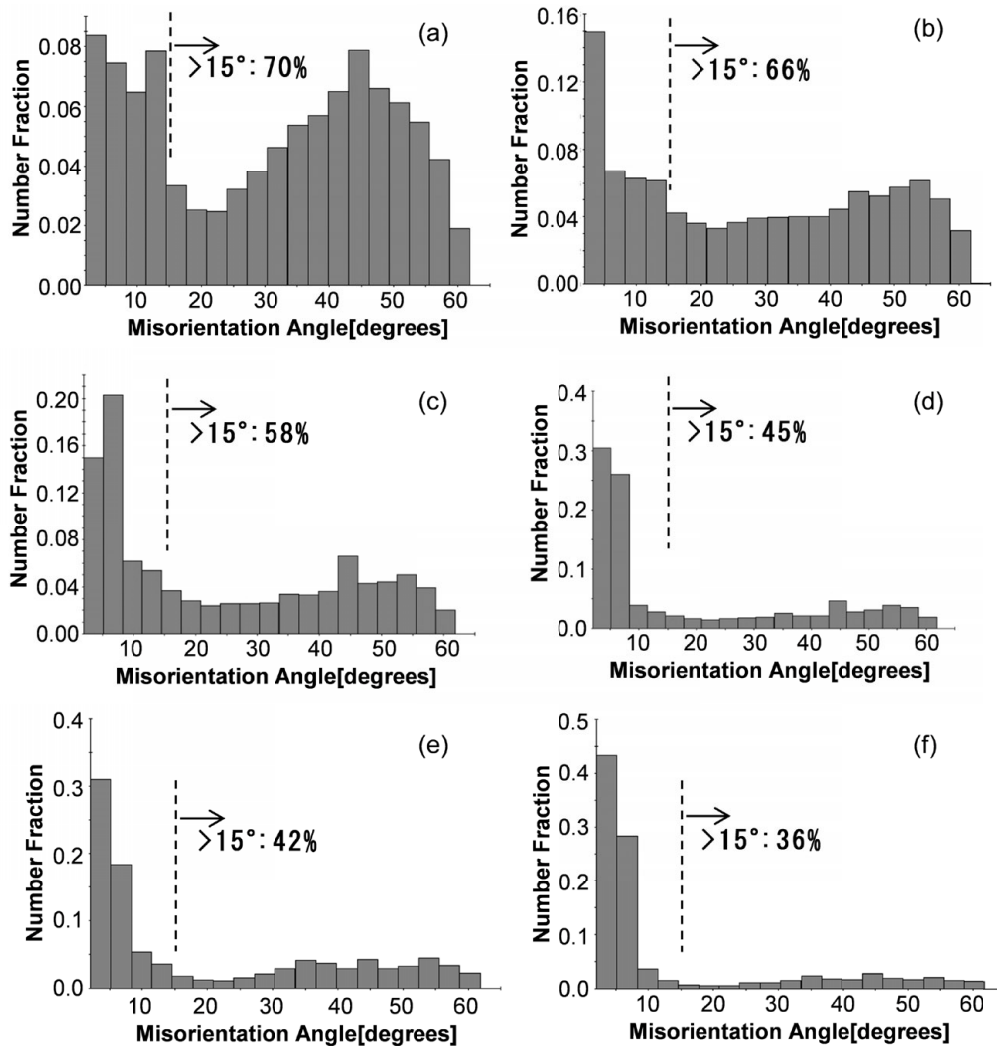


Fig. 5 Misorientation distributions of the grain boundaries obtained by EBSD measurement for the specimens ARB-processed and subsequently annealed at various temperatures. (a) The as-ARB processed, (b) 200°C, (c) 250°C, (d) 300°C, (e) 400°C, (f) 500°C

Acknowledgements

This work was supported by a National Research Foundation of Korea (NRF) grant, funded by the Korea government (MSIT) (No. 2022R1A2C1012426).

REFERENCES

- [1] S.W. Park, Y.W. Song, J.Y. Yeo, S.Y. Han, H.J. Choi, *J. Power Mater.* **30** (3), 203 (2023).
- [2] J.A. Lee, J.H. Choe, H.S. Kim, *J. Power Mater.* **30** (3), 255 (2023).
- [3] Y. Saito, N. Tsuji, H. Utsunomiya, T. Sakai, R.G. Hong, *Scrip. Mater.* **39**, 1221 (1998).
- [4] Y. Saito, H. Utsunomiya, N. Tsuji, T. Sakai, *Acta. Mater.* **47**, 579 (1999).
- [5] S.H. Lee, Y. Saito, T. Sakai, H. Utsunomiya, *Mater. Sci. Eng.* **A325**, 228 (2002).
- [6] S.H. Lee, H. Utsunomiya, T. Sakai, *Mater. Trans.* **45**, 2177 (2004).
- [7] S.H. Lee, *J. Kor. Inst. Met. & Mater.* **43** (12), 786 (2005).
- [8] S.H. Lee, C.H. Lee, S.Z. Han, C.Y. Lim, *J. Nanosci. and Nanotech.* **6**, 3661 (2006).
- [9] S.H. Lee, C.H. Lee, S.J. Yoon, S.Z. Han, C.Y. Lim, *J. Nanosci. and Nanotech.* **7**, 3872 (2007).
- [10] N. Takata, S.H. Lee, C.Y. Lim, S.S. Kim, N. Tsuji, *J. Nanosci. and Nanotech.* **7**, 3985 (2007).
- [11] S.H. Lee, H.W. Kim, C.Y. Lim, *J. Nanosci. and Nanotech.* **10**, 3389 (2010).
- [12] M. Eizadjou, A. Kazemi Talachi, H. Danesh Manesh, H. Shakir Shahabi, K. Janghorban, *Composites Sci. and Tech.* **68**, 2003 (2008).
- [13] Ming-Che Chen, Chih-Chun Hsieh, Weite Wu, *Met. Mater. Int.* **13** (3), 201 (2007).
- [14] Guanghui Min, J.M. Lee, S.B. Kang, H. W. Kim, *Mater. Letters* **60**, 3255 (2006).
- [15] S.H. Lee, C.S. Kang, *Korean J. Met. Mater.* **49** (11), 893 (2011).
- [16] S.H. Lee, J.H. Kim, *Korean J. Met. Mater.* **51** (4), 251 (2013).
- [17] S.H. Lee, J.H. Kim, *J. Nanosci. and Nanotech.* **15**, 459 (2015).
- [18] S.H. Lee, *Arch. Metall. Mater.* **65**, 1093 (2020).
- [19] S.H. Jo, S.H. Lee, *Arch. Metall. Mater.* **66**, 765 (2021).
- [20] S.H. Jo, S.H. Lee, *Korean J. Mater. Res.* **32** (2), 72 (2022).